

Inversion of coseismic deformation due to the 8th February 2016, Mw 4.2 earthquake at Los Humeros (Mexico) inferred from DInSAR

Eszter Békési¹, Peter A. Fokker^{1,2}, Joana E. Martins^{2,3}, Jan-Diederik van Wees^{1,2}

¹ Department of Earth Sciences, Utrecht University, Princetonlaan 4, 3584 CB Utrecht, Netherlands

² TNO Utrecht, Princetonlaan 6, 3584 CB Utrecht, Netherlands

³ TU Delft Faculty Of Civil Engineering and Geosciences, Stevinweg 1, 2628 CN Delft

e.bekesi@uu.nl

Keywords: Induced Seismicity, DInSAR, Los Humeros Geothermal Field

ABSTRACT

On the 8th of February 2016, a Mw 4.2 earthquake was detected inside the Los Humeros caldera, located in the eastern sector of the Trans-Mexican Volcanic Belt. The event occurred after a sharp increase in the injection rate at the Los Humeros Geothermal Field and it was recorded by the seismic monitoring network of the power plant. The earthquake was felt by the local population and it caused damage in the power plant infrastructure. The focal mechanism solution of a previous study based on seismological data shows a reverse movement with a minor left-lateral component: Mw=4.2, depth=1500m, strike=169°, dip=61°, rake=42°.

We have performed a geodetic and geomechanical analysis of the seismic source event based on ground deformation inferred from DInSAR. We used ascending and descending Sentinel-1 differential interferograms to retrieve the horizontal and vertical components of the co-seismic deformation. Subsequently, we inverted the estimated deformation to obtain the solution of an activated fault using the Okada model. These results shed light on the geomechanical aspects of the event and can help to understand the effects of field operations interacting with pre-existing structural features and active tectonic processes in the Los Humeros caldera.

1. INTRODUCTION

The Differential Interferometric Synthetic Aperture Radar (DInSAR) technique by exploiting high-resolution satellite radar images has become an important tool for monitoring deformation of the Earth's surface [Hanssen, 2001; Ferretti, 2014]. The DInSAR technique is widely used for mapping different geophysical phenomena such as earthquakes, volcanos, landslides, and ground deformation associated with, for instance, subsurface exploration processes [e.g. Atzori et al, 2009]. Sentinel-1 satellites operating on C-band by the European Space Agency

provide regular observations with a temporal resolution of 6 to 12 days, facilitating the monitoring of surface movements with short revisiting times.

This study focuses on the coseismic deformation due to a seismic event on the 8th of February 2016 at the Los Humeros Geothermal field (LHGF) (Fig. 1). The LHGF is among the largest geothermal fields in Mexico, producing ~68.6 MW operated by the national Mexican Electrical company (Comisión Federal de Electricidad, CFE). The LHGF is located inside the quaternary Los Humeros Caldera system, forming the easternmost caldera of the Trans-Mexican Volcanic Belt (Fig. 1) The geothermal reservoir is built up by pre-caldera andesites of Miocene age (Ferriz and Mahood 1984), situated at ~1500 m depth, with an average thickness of ~1000 m (e.g. Carrasco-Núñez et al. 2017). The geothermal activity is controlled by NNW-SSE to E-W striking structures located inside the caldera (Fig. 1). These active faults induce secondary permeability, providing the path of geothermal fluids associated with active caldera resurgence processes (e.g. Norini et al. 2015).

The 8 February 2016 earthquake originated along the trace of the Los Humeros fault, which is one of the main structures of the caldera floor. The event occurred after a sharp increase in the injection rate at the H-29 well, located north of the epicentre (Fig. 1).

Previous work on the seismic event based on seismological data was performed by Lermo Samaniego et al. (2016). Additionally, DInSAR monitoring and forward modelling has been conducted by Santos-Basurto et al. (2018). The focal mechanism solutions after Lermo Samaniego et al. (2016) are marked by high uncertainties as only the polarities of the P-wave arrivals at the vertical components of five seismic stations were used for the inversion. The coseismic deformation was previously mapped by Santos-Basurto et al. (2018) using the same interferograms as we produced in this study. However, the misfits of the forward model of Santos-Basurto et al. (2018) are in the same order of magnitude as the

DInSAR observations themselves, motivating us to perform this study.

We have attempted to resolve the source parameters of the earthquake to better explain the observed ground deformation pattern. To this end we first mapped the ground deformation through DInSAR using ascending and descending Sentinel-1 images. We then inverted the ground movements for an activated fault solution aiming to retrieve the geomechanical parameters of the event and to understand interactions between field operations and pre-existing structural features and tectonic processes. By the inversion of the surface movements we intend to understand fault reactivation which can reveal further characteristics of the geothermal field.

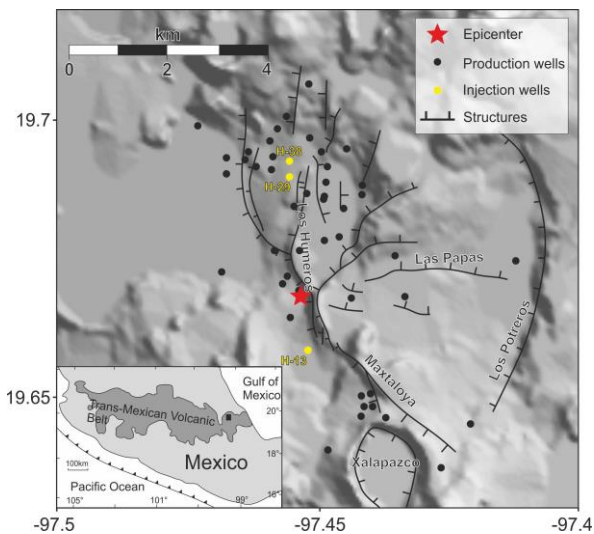


Figure 1: Major faults, caldera rims, and the location of the wells at the Los Humeros Geothermal Field modified after Norini et al. (2015) and Carrasco-Núñez et al. (2017). The red star indicates the epicentre of the 8 February 2016, Mw 4.2 earthquake after Lermo Samaniego et al. (2016).

2. INSAR DATA AND PROCESSING

We processed Sentinel-1 (S-1) radar images acquired in wide-swath. We used the images of 29 January 2016 and 10 February 2016 for the ascending interferogram. The descending interferogram was processed using the SAR images acquired on 7 February 2016 and on 19 February 2016.

The interferometric processing was performed using the GAMMA software (Wegmüller and Werner 1997). S-1 images are built up by several bursts, for which the processing starts with the selection of overlapping bursts of the image pairs and it is followed by the coregistration of the slave image to the master geometry. We used an external Digital Elevation Model (DEM) of 30-m resolution from the Shuttle Radar Topography Mission (SRTM) to compute the topographic phase for both image pairs, and we removed it from the computed interferograms. Afterwards, we applied an adaptive filtering and performed the phase unwrapping to compute

displacements relative to the satellite line-of-sight (LOS). For the modelling we masked out the area near the surface rupture of the fault due to the high potential for unwrapping errors resulting from the lack of coherence.

3. GEODETIC MODELING

We inverted the ascending and descending interferograms for a fault solution with uniform slip using the Okada model (Okada 1985). We used the freely available MATLAB-based Geodetic Bayesian Inversion Software (GBIS, <https://comet.nerc.ac.uk/gbis/>) for the parameter estimation procedure. GBIS adopts a Bayesian approach for rapid inversion of multiple geodetic datasets to characterize the posterior probability density functions (PDFs) of source parameters and associated uncertainties. The PDFs are sampled by a Markov Chain Monte Carlo method with automatic step size selection using the Metropolis Hastings algorithm (Hastings 1970). More details on the methodology can be found in Bagnardi and Hooper (2018).

We performed the modelling using the ascending and descending interferograms separately (Model 1 and Model 2, respectively) and with the combination of the two datasets (Model 3). We inverted the single datasets with the motivation to map the source parameters that better fit with the ascending and descending data separately. Prior to the modelling, InSAR data were subsampled using an adaptive quadtree sampling algorithm (Decriem et al. 2010). This was necessary due to the high density of the PS points, which would require a computationally expensive inversion. The algorithm works as areas with large phase variance are subdivided more finely, and areas with low variance remain coarser. Our datasets covering approximately 8x8 km are resampled to 223 and 217 data points for the ascending and descending interferograms, respectively (Fig. 2).

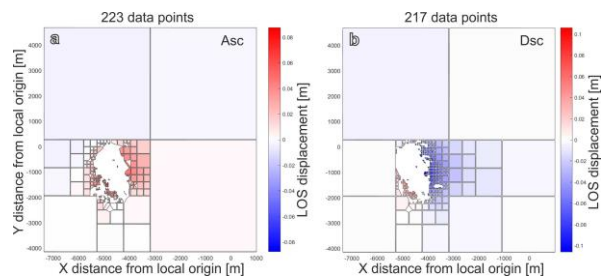


Figure 2: Subsamped unwrapped InSAR datasets for ascending (a) and descending (b) satellite passes obtained by the quadtree algorithm. The colouring corresponds to displacements relative to the satellite LOS (positive values: movements towards the satellite, negative values: movement away from the satellite).

The inversion targeted a forward model for a rectangular dislocation with nine adjustable parameters. The source parameters are the length, width, depth of the midpoint of the upper edge, dip angle (negative due to dipping to the west), strike

(clockwise from north), X and Y coordinates of the midpoint of the upper edge, and the amount of the uniform slip in the strike and dip directions. We selected lower and upper bounds for the source parameters according to prior information about the activated fault based on the observed ground movement pattern and previous studies including geological mapping (e.g. Norini et al. 2015) and seismological data (Lermo Samaniego et al. 2016). Constraints on the magnitude of slip were set conforming to the amplitude of surface movements inferred from the InSAR data. Based on the ascending and descending interferograms, the vertical and eastern components of the slip are approximately 0.18 m and 0.06 m. To infer the northern component of the displacement, another interferogram with different look direction is required. Bounds were chosen identical for all models and are listed in Table 1.

4. RESULTS

Our modelling results of the surface deformation due to the 8 February 2016 earthquake at the LHGF are

summarized in Table 1 and Figure 3. Surface movements predicted by the three models are consistent with a NNW-SSE-strike, westward dipping reverse fault with minor strike-slip component (table 1). However, the geometry of the fault varies for each model. In case of Model 1 and Model 3, the fault extends from the surface down to 1100-1300 m depth. Model 2 predicts a vertical fault plane with half of the width of the other two models, where the top edge is located at almost 500 m depth. The dip is significantly smaller for Model 1 and Model 3, with $\sim 53^\circ$ and $\sim 59^\circ$, respectively. Due to the smaller area of the fault plane in Model 2, the slip in dip direction is two and three times larger with respect to Model 1 and Model 3.

The models calibrated with a single dataset (Model 1, Figure 2b, and Model 2, Figure 2g) show very good fit with the ascending (Figure 2a) and descending (Figure 2f) interferograms separately. In case of the two datasets inverted simultaneously (Model 3, Figure 2d,i), misfits increase (Figure 2e,j), especially with the descending data.

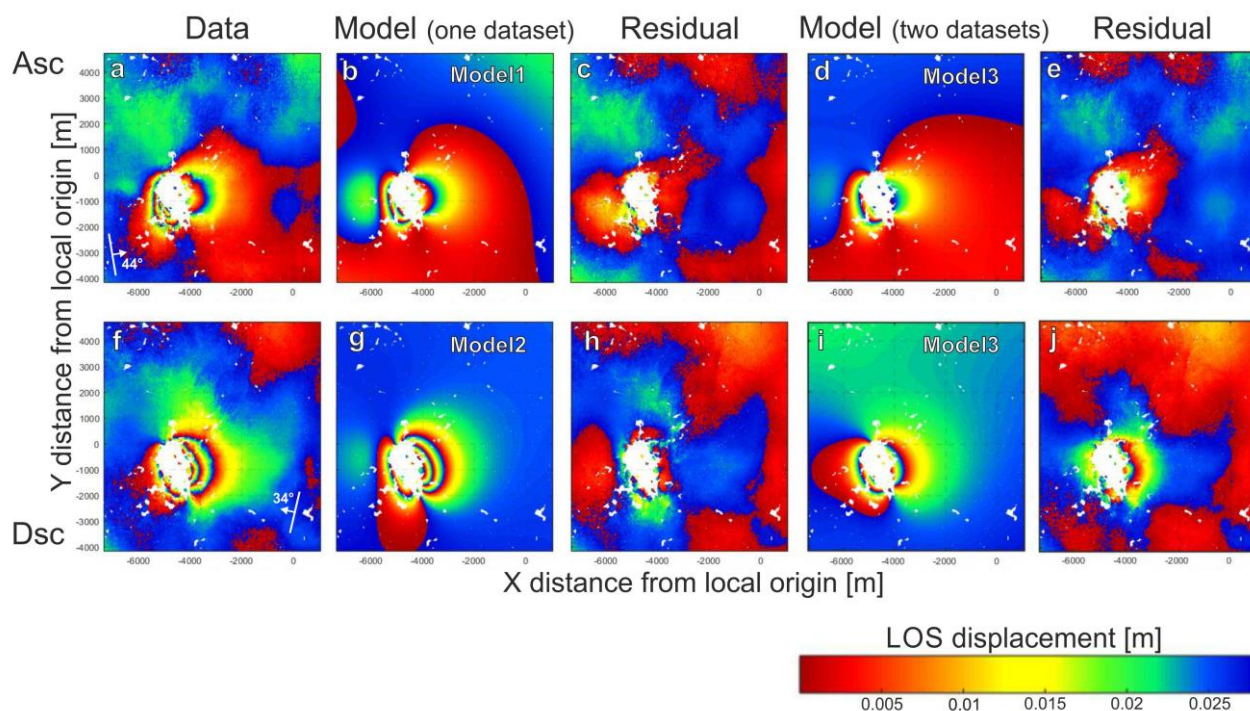


Figure 3: Observed (a, f), modeled (b, d, g, i), and residual (c, e, h, j) displacements in the LOS direction for ascending (top) and descending (bottom) satellite passes, mapping the coseismic deformation of the 8 February 2016 earthquake. Arrows in a and f indicate the flight direction of the satellite and the look direction with the corresponding incidence angles. Model 1 and Model 2 are obtained by the inversion of the ascending and descending interferograms separately. For Model 3 the two interferograms were used simultaneously.

	Total Model Range		Model 1	Model 2	Model 3
	Lower	Upper	Optimal (2.5% – 97.5%)	Optimal (2.5% – 97.5%)	Optimal (2.5% – 97.5%)
Top Depth [m]	0	2000	2.08 (0.034 – 3.82)	485.03 (485.03 – 485.03)	0.89 (0.26 – 3.86)

Dip [°]	-90	-45	-52.57 (-54.09 – -51.40)	-90.00 (-90.00 – -90.00)	-58.92 (-60.67 – -58.08)
Strike [°]	270	360	341.74 (341.14 – 341.89)	334.72 (334.72 – 334.72)	339.74 (339.66 – 340.48)
Length [m]	1000	2500	1489.13 (1455.18 – 1512.77)	1814.51 (1814.51 – 1814.51)	1655.46 (1632.21 – 1678.68)
Width [m]	500	2000	1141.72 (1108.34 – 1185.52)	517.35 (517.35 – 517.35)	1301.08 (1249.40 – 1372.38)
X center [m]	-4650	-4450	-4534.55 (-4538.58 – -4533.69)	-4631.75 (-4631.75 – -4631.75)	-4529.56 (-4535.18 – -4529.14)
Y center [m]	-1000	-800	-865.54 (-867.06 – -853.84)	-992.72 (-992.72 – -992.71)	-844.09 (-844.73 – -839.78)
Strike slip [m]	-0.5	0.5	-0.055 (-0.072 – -0.052)	0.0720 (0.035 – 0.128)	-0.052 (-0.062 – -0.045)
Dip slip [m]	-2.0	2.0	-0.284 (-0.296 – -0.271)	-0.638 (-0.652 – -0.614)	-0.180 (-0.184 – -0.173)

Table 1: Prior values and inversion results of the source parameters of the 8 February 2016 earthquake at Los Humeros. 2.5 and 97.5 percentiles of posterior probability density functions of the fault parameters are reported. For Model 1 and Model 2 we employed the ascending and descending datasets respectively. Model 3 was constructed based on the joint inversion of the two interferograms. Note that the strike and dip ranges are selected in order to fix the position of the midpoint of the top edge of the fault plane (see Bagnardi and Hooper 2018).

5. DISCUSSION AND CONCLUSIONS

We processed ascending and descending Sentinel-1 interferograms to map the coseismic deformation due to the 8 February 2016 earthquake that occurred at the LHGF. We inverted the interferograms for an activated fault solution using the datasets separately (Model 1 and Model 2) and jointly (Model 3). Our models yielded significantly different source parameters, especially when the descending dataset is used (Model 2). This leads to the conclusion that using either ascending or descending data can yield misleadingly good fits and misleadingly well-constrained parameter estimates. The combination of the data sets provides for essential additional information.

Our model calibrated jointly with the two interferograms (Model 3) shows misfits up to 30 mm with the descending data. These misfits suggest that the models are inaccurate. We think the source of the inaccuracy is in the assumption of a single fault plane with uniform slip. Despite the inaccuracy, however, all models locate the activation of the fault at shallow depth: no activation was predicted below ~1200m depth. This implies that the earthquake most likely originated in the top of the reservoir. Additionally, all models predict a reverse movement along the trace of the Los Humeros fault. This fault was previously mapped as a normal fault associated with the resurgence of the caldera floor east of the fault (e.g. Norini et al. 2015), suggesting reactivation with opposite kinematics. This reactivation may imply the cessation of resurgence processes inside the caldera or alternatively the tilting of a trapdoor block (e.g. Acocella 2007).

The InSAR observations are in good agreement with the coseismic deformation mapped by Santos-Basurto et al. (2018). However, their forward model shows misfits up to two times larger than in our Model 3.

The most important model parameters are the depth of the centre of the fault plane, the fault orientation and the rake of the event. The fault orientation and event rake are in good agreement, but the difference in depth is large (Model3: depth of the center of the fault plane=558m, strike=160°, dip=59°, rake=75°; seismological data: Mw=4.2, depth=1500m, strike=169°, dip=61°, rake=42°, Lermo Samaniego et al. 2016). This mismatch may originate from the uncertainty assigned to the focal mechanism inversion. Additionally, our model is based on a uniform slip along a rectangular plane in an elastic half-space, while the fault pattern inside the Los Humeros caldera is much more complex and the subsurface is heterogeneous. Considering the uncertainties of our models, we conclude that they are not entirely capable of explaining the observed ground deformation pattern. The joint deployment of ascending and descending InSAR data has shown that further research, taking into account the complexity in the subsurface, is crucial for a quantitative understanding. However, the present study has given a good estimate of the reactivated fault orientation and rake, and it has set the direction in which to search to reveal the other source parameters. Such understanding can then be used to develop understanding and quantification of the connection between geothermal operations and induced seismicity.

REFERENCES

- Acocella, V.: Understanding caldera structure and development: An overview of analogue models compared to natural calderas. *Earth-Science Reviews*, (2007), 85(3-4), 125-160.
- Atzori, S., Hunstad, I., Chini, M., Salvi, S., Tolomei, C., Bignami, C., ... & Boschi, E. (2009). Finite fault inversion of DInSAR coseismic displacement of the 2009 L'Aquila earthquake (central Italy). *Geophysical Research Letters*, 36(15).

- Bagnardi, M., Hooper, A.: Inversion of surface deformation data for rapid estimates of source parameters and uncertainties: A Bayesian approach. *Geochemistry, Geophysics, Geosystems*, (2018), 19(7), 2194-2211.
- Carrasco-Núñez, G., López-Martínez, M., Hernández, J., & Vargas, V.: Subsurface stratigraphy and its correlation with the surficial geology at Los Humeros geothermal field, eastern Trans-Mexican Volcanic Belt. *Geothermics*, (2017), 67, 1-17.
- Decriem, J., Árnadóttir, T., Hooper, A., Geirsson, H., Sigmundsson, F., Keiding, M., et al.: The 2008 May 29 earthquake doublet in SW Iceland. *Geophysical Journal International*, (2010), 181(2), 1128–1146.
- Ferretti, A. (2014). Satellite InSAR data: reservoir monitoring from space. EAGE publications.
- Ferriz, H., Mahood, G.: Eruption rates and compositional trends at LosHumeros volcanic center, Puebla, Mexico, *J. Geophys. Res.*, (1984), 89 (B10),8511–8524.
- Hanssen, R. F. (2001). Radar interferometry: data interpretation and error analysis (Vol. 2). Springer Science & Business Media.
- Hastings, W. K.: Monte Carlo sampling methods using Markov chains and their applications. *Biometrika*, (1970), 57(1), 97–109.
- Lermo Samaniego, J. F., Lorenzo, C., Antayhua, Y., Ramos, E., & Jiménez, N.: Sísmica pasiva en el campo geotérmico de los Humeros, Puebla-México y su relación con los pozos inyectores. *XVIII Congreso Peruano de Geología 2016*, Sociedad Geológica del Perú, Lima, Perú, (2016), p. 5.
- Norini, G., Groppelli, G., Sulpizio, R., Carrasco-Núñez, G., Davila-Harris, P., Pelliccioli, C., Zucca, F., De Franco, R.: Structural analysis and thermal remote sensing of the Los Humeros Volcanic Complex: implications for volcano structure andgeothermal exploration. *J. Volcanol. Geotherm. Res.*, (2015), 301, 221–237.
- Okada, Y.: Surface deformation due to shear and tensile faults in a half-space. *Bulletin of the seismological society of America*, (1985), 75(4), 1135-1154.
- Santos-Basurto, R., Sarychikhina, O., López-Quiroz, P., Norini, G., Carrasco-Núñez, G.: The Mw 4.2 (February 8th, 2016) earthquake detected inside of Los Humeros caldera, Puebla-Mexico, by means of DInSAR. *European Geosciences Union 2018*, Vienna, Austria (2018), poster 18431.
- Wegmüller, U., Werner, C.: Gamma SAR processor and interferometry software. *Proceedings of the 3rd ERS Symposium 1997*, Florence, Italy, (1997), 14–21.

Acknowledgements

The research leading to these results has received funding from the GEMex Project, funded by the European Union’s Horizon 2020 research and innovation programme under grant agreement No. 727550.

We thank the Mexican Electrical company (Comisión Federal de Electricidad, CFE) for access to relevant field and production data in the framework of the GEMex project.